

Experimental Evidence of Excited Multicharged Atomic Fragments Coming from Laser-Induced Coulomb Explosion of Molecules

L. Quaglia and C. Cornaggia

CEA Saclay, Division des Sciences de la Matière, Service des Photons, Atomes et Molécules, Bâtiment 522, F-91191 Gif-sur-Yvette, France

(Received 6 January 2000)

Direct experimental evidence is presented for the production of excited multicharged atomic fragments in the laser-induced Coulomb explosion of molecules. The comparison of the fluorescence signals of several atomic and molecular species shows that the excited fragments come from transient excited multicharged molecules. The atomic fluorescence spectra recorded with NH_3 , N_2 , and N_2O , in the 50–120 nm wavelength range, show that the excitation increases noticeably from NH_3 to N_2O . This effect is interpreted in terms of the initial electronic configuration, which favors a stronger excitation when the electronic density is more delocalized on the molecular nuclear structure.

PACS numbers: 33.80.Rv, 33.80.Eh, 42.50.Vk

Laser-induced Coulomb explosion of molecules is currently studied using ion time-of-flight mass spectrometry, in order to determine the fragmentation channels and the associated kinetic energy releases [1]. The experimental results have shed some light on the molecular multi-ionization processes in strong laser fields, and major advances have appeared during the last few years in the theoretical understanding of the laser-molecule coupling [2–6]. However, the degrees of excitation of the detected multicharged atomic fragments remain largely unknown. This Letter aims to report the first experimental evidence for excited multicharged fragments for molecules such as NH_3 , N_2 , and N_2O using conventional photon spectroscopy. Similar results were recorded with other molecules such as O_2 or CO_2 and will be reported in a longer paper with a more detailed analysis.

These results are important for the basic understanding of laser-induced molecular multiple ionization. Until now, the transient molecular multicharged ions are identified through the multifragmentation channels, which are studied measuring the fragments' charge states and kinetic energies. However, these types of measurements are not sufficient in order to know the internal energy of the multicharged molecule, since the fragmentation kinetic energy releases allow us to know only the excess energies above the different dissociation limits. In consequence, the occurrence of excited molecular states can be investigated only using photon spectroscopy. Besides their fundamental aspects, these processes are of practical importance for radiation sources in the extreme ultraviolet range and might lead to specific inversion diagrams for light amplification.

The fluorescence photon detection is known to be much less efficient than the ion detection. In particular, the photon emission spectra are recorded in the 10^{-4} Torr range, which is a relatively high pressure in comparison with the pressure range used for the time-of-flight ion mass spectra. In consequence, the first issue of these experiments is to avoid any collective effects in order to get the unimolecular

response, without any electron impact excitation or recombination effects. The overall unresolved photon signals are first recorded at very low pressures in the 10^{-9} – 10^{-5} Torr range. In each pressure range, the linear pressure dependence of the signal ensures a unimolecular response without any collective effects. The second point that will be addressed concerns the origin of the fragments' excited states. These states might come from the excited states of the transient multicharged molecule or from a subsequent laser excitation of atomic fragments following molecular Coulomb explosion. This point is discussed in relationship with the measured ion kinetic energies and shows that the origin of the photon signals has to be searched in excited molecular states.

The experiments were performed using the Saclay LUCA laser facility (LUCA for Laser Ultra-Court Accordable). The pulse duration is 60 fs at $\lambda = 800$ nm, and an energy up to 80 mJ was used in the experiments. The laser beam is focused at $F/4$ using a fused silica lens with focal length $F = +200$ mm, and the spot size has been measured to be $S_0 = 2.5 \times 10^{-6}$ cm² at the best focus. The molecular relaxation is studied using two separate experimental setups. The first one is a Wiley and McLaren ion spectrometer with a 780 mm long drift tube [7]. Figure 1 presents the ion time-of-flight mass spectrum recorded with the N_2 molecule. Because of the high laser intensity, the very low gas pressure $p(\text{N}_2) = 10^{-9}$ Torr is sufficient to record the ion signals, and in consequence the ions H^+ , H_2^+ , H_2O^+ , and O^{Z+} ($Z = 1, 2, 3$) coming from the background pressure $p = 3 \times 10^{-10}$ Torr are also clearly identified in the time-of-flight mass spectrum. Charge states up to $Z = 5$ for the N^{Z+} ions were detected in the 10^{16} – 5×10^{17} W/cm² intensity range. For charge states up to $Z = 3$, the kinetic energy releases are identical to measurements performed at lower laser intensities in the 10^{15} W/cm² intensity range [8]. Moreover, the fragmentation channels remain identical at larger laser intensities, and no postdissociative ionization has been

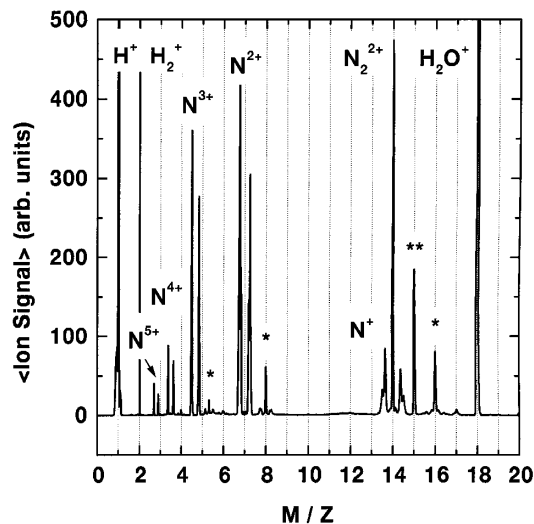


FIG. 1. Time-of-flight mass spectrum of N_2 recorded at $I = 2 \times 10^{17}$ W/cm 2 , $\lambda = 800$ nm, and $p(N_2) = 10^{-9}$ Torr. The laser polarization direction is parallel to the spectrometer axis. Each N^{Z+} ion peak presents a double peak structure because of ions ejected towards the detector and away from the detector. The ion peaks coming from the background pressure are also indicated: the (*) peaks are O^{Z+} ($Z = 1, 2, 3$) ion peaks and the (**) peak at $M/Z = 15$ might be a CH_3^+ ion peak coming from heavy residual hydrocarbon molecules.

detected for channels up to $N^{3+} + N^{3+}$, where comparisons are possible with experiments performed at lower laser intensities [8]. Higher peak laser intensities than in Ref. [8] are used in order to increase the interaction volume and to get a sufficient photon signal allowing us to work with low gas pressures.

The photon emission is investigated using two methods. The first type of experiment is performed in the high vacuum chamber that contains the ion time-of-flight spectrometer. In the opposite direction of the long drift tube, the photon signals are recorded through three high 90% transparency grids on a 40 mm effective diameter micro-channel plate detector, located at 150 mm from the laser focus. The function of the grids is to detect ions, electrons, or photons. In this last case, high voltages were applied on the grids to reject any high energy electron signal. Moreover, the photon signals are simultaneous with the laser signal detected with a fast photodiode. The geometric efficiency for photon collection is $\Delta\Omega/4\pi = 4 \times 10^{-3}$. Figure 2 represents the photon signals as functions of the gas pressure in the 10^{-9} – 10^{-5} Torr pressure range for different atomic and molecular species. For each gas, the linear dependence of the photon signal shows that the light emission is a unimolecular process without any collective effects.

A second experimental setup was used to record the photon spectra in the 50–150 nm wavelength range. It includes an interaction chamber, where the laser is focused using the same optical compounds as for the ion spectrometer, a photon spectrometer equipped with

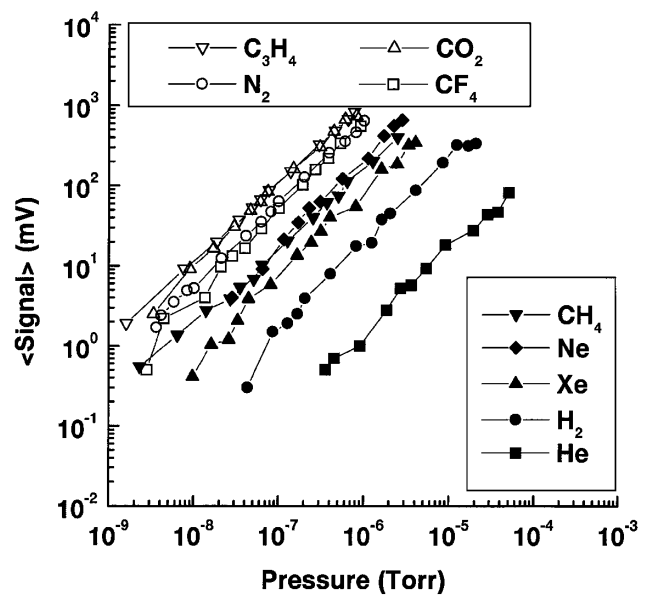


FIG. 2. Pressure dependence of the photon signals for different atomic and molecular gases: He, Ne, Xe, H_2 , CH_4 , CF_4 , N_2 , CO_2 , and C_3H_4 .

a 275 line/mm toroidal grating, and an electron multiplier built with Cu-Be dynodes to record the signals. The spectrometer has been calibrated using a helium lamp. Using 0.25 mm wide slits, the resolution is given at $\lambda(HeI\alpha) = 58.4$ nm by $\Delta\lambda = 1.2$ nm. Even with relatively large slits, the geometrical collection efficiency is very low, $\Delta\Omega/4\pi = 8 \times 10^{-6}$, and relatively high pressures in the 10^{-5} – 5×10^{-4} Torr range were necessary to record the photon spectra. Figure 3 represents the emission spectra recorded with NH_3 , N_2 , and N_2O at $p = 5 \times 10^{-4}$ Torr. Only the N^{Z+} ($Z = 1, 2, 3$) lines have been reported in Table I for a comparison between the different gases' efficiencies. In the case of NH_3 , no lines were detected from excited H atoms, and, for N_2O , lines from O^{Z+} ($Z = 1, 2, 3$) have also been detected and will be reported in a longer paper. Finally the pressure dependence of several atomic nitrogen lines is reported in Fig. 4. The linear dependence in the 10^{-4} Torr range shows again that the emission lines come from unimolecular processes without any collective effects' contributions.

Except for H_2 in Fig. 2, the fluorescence signals coming from molecules such as C_3H_4 , N_2 , or CF_4 are higher than the fluorescence signals coming from He, Ne, and Xe atoms. The CH_4 molecule exhibits the same efficiency as the Ne atom. These observations rule out any processes coming from the laser excitation of the fragments following the molecular Coulomb explosion. In this last case, atomic species should also be sensitive to the laser excitation and the corresponding multicharged atomic ions would be expected to fluoresce as well. The molecular excitation that is responsible for the fragment fluorescence signals is also significant in the comparison of several molecular responses. For instance, the CF_4 molecule is

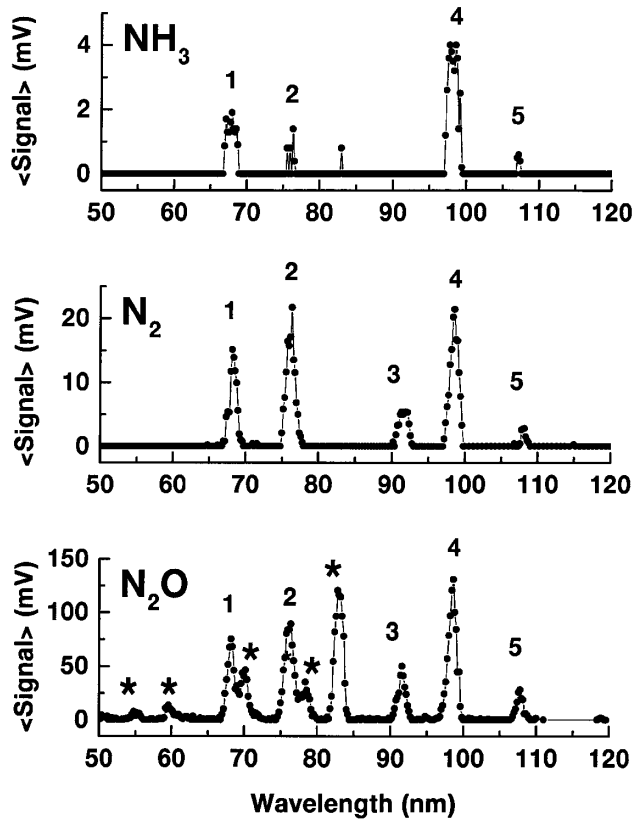


FIG. 3. Photon emission spectra recorded with NH_3 , N_2 , and N_2O at $\lambda = 800$ nm, $I = 2 \times 10^{17}$ W/cm², and $p = 5 \times 10^{-4}$ Torr. The atomic nitrogen lines No1–No5 are identified in Table I. The atomic oxygen lines of N_2O are indicated by the (*) symbol.

more efficient than the CH_4 molecule, because the F atoms and ions contribute to the photon signals more efficiently than the H atoms. Indeed, no H-Lyman- α or - β lines were detected in the 10^{-4} Torr range. However, the N_2 and CF_4 total efficiencies are comparable in Fig. 2, although N_2 and CF_4 have, respectively, two and five emitting atoms.

The molecular response is reported in more detail for NH_3 , N_2 , and N_2O in Fig. 3. Five lines coming from excited N^{Z+} ($Z = 1, 2, 3$) are detected and are identified in Table I. Lines No2 and No3 correspond to several transitions that cannot be resolved due to the spectrometer low

resolution. The N^{2+} ion appears to be the major precursor for the photon emission. This statement is in good qualitative agreement with the ion time-of-flight mass spectrum of N_2 represented in Fig. 1, where the N^{2+} signal is the largest one. The same behavior is also observed for NH_3 and N_2O . In Fig. 3, the vertical units are identical for the three molecules, and the photon signals are much weaker for NH_3 than for N_2 and N_2O . In particular, line No3 is not detected for NH_3 , and line No2 is weaker than line No1 for this molecule, while this is not the case in N_2 and N_2O .

The line intensities are summarized in Table I for each gas at the same pressure $p = 5 \times 10^{-4}$ Torr. These intensities are normalized to the number of nitrogen atoms within each molecule, since Coulomb explosion produces only one N^{Z+} ion for NH_3 , and two N^{Z+} and $\text{N}^{Z'+}$ ions for N_2 and N_2O . Table I shows that the photon emission efficiency increases noticeably from NH_3 to N_2O . This observation is another signature of the molecular origin of the fluorescence spectra. Indeed, the laser excitation of fragments following Coulomb explosion would be expected to be equivalent for the three molecules.

The main conclusion of our experimental results shows that the excited fragments come from excited transient multicharged molecules, since postdissociative excitations do not play a significant role. This statement is established in relationship to measurements performed with atoms, with different molecular species, and finally is confirmed by the absence of postdissociative ionization in Coulomb explosion experiments performed with femtosecond pulse duration lasers. The molecular explosion takes a few tens of femtoseconds and is very fast in comparison with the atomic fragment excited state lifetimes, which are in the (sub-)nanosecond range. In consequence, the photon emission concerns mainly the fragments, while the transient molecular ion has very little time to emit a photon. The second important conclusion concerns the very different photon emission efficiency depending upon the atomic or molecular species as can be seen in Fig. 2 and in Table I. The case of molecules such as CH_4 or NH_3 is much closer to the atomic Ne case than diatomic or triatomic molecules built with equivalent C, N, O, or F atoms. For XH_n ($X = \text{C}, \text{N}, \text{O}$) molecules, the electronic density is localized mainly on the X atom. The very fast departure of

TABLE I. Nitrogen emission lines detected in NH_3 , N_2 , and N_2O . The line numbers refer to the labels of Fig. 3. The line intensities $\text{Int}(\text{NH}_3)$, $\text{Int}(\text{N}_2)$, and $\text{Int}(\text{N}_2\text{O})$ are normalized to the number of nitrogen atom within each molecule.

Line No	Ion	Transition	$\text{Int}(\text{NH}_3)$	$\text{Int}(\text{N}_2)$	$\text{Int}(\text{N}_2\text{O})$
1	N^{2+}	$2s2p^2\ ^2P[18.1 \text{ eV}] \rightarrow 2s^2(^1S)2p^2\ ^2P^0[0 \text{ eV}]$	1.2	7.6	37.4
2	N^{2+}	$2s2p^2\ ^2S[16.3 \text{ eV}] \rightarrow 2s^2(^1S)2p^2\ ^2P^0[0 \text{ eV}]$			
	N^{2+}	$2p^3\ ^4S^0[23.2 \text{ eV}] \rightarrow 2s2p^2\ ^4P[7.1 \text{ eV}]$	0.9	10.9	44.5
	N^+	$2s(^2S)2p^3\ ^1D^0[17.9 \text{ eV}] \rightarrow 2s^2(^1S)2p^2\ ^1D[0 \text{ eV}]$			
3	N^+	$2s(^2S)2p^3\ ^3P^0[13.5 \text{ eV}] \rightarrow 2s^2(^1S)2p^2\ ^3P[0 \text{ eV}]$	0	2.6	25
	N^{3+}	$2p^2\ ^3P[21.8 \text{ eV}] \rightarrow 2s(^2S)2p^3\ ^3P^0[8.3 \text{ eV}]$			
4	N^{2+}	$2s2p^2\ ^2D[12.5 \text{ eV}] \rightarrow 2s^2(^1S)2p^2\ ^2P^0[0 \text{ eV}]$	2.6	10.7	65.4
5	N^+	$2s(^2S)2p^3\ ^3D^0[11.4 \text{ eV}] \rightarrow 2s^2(^1S)2p^2\ ^3P[0 \text{ eV}]$	0.4	2.6	25

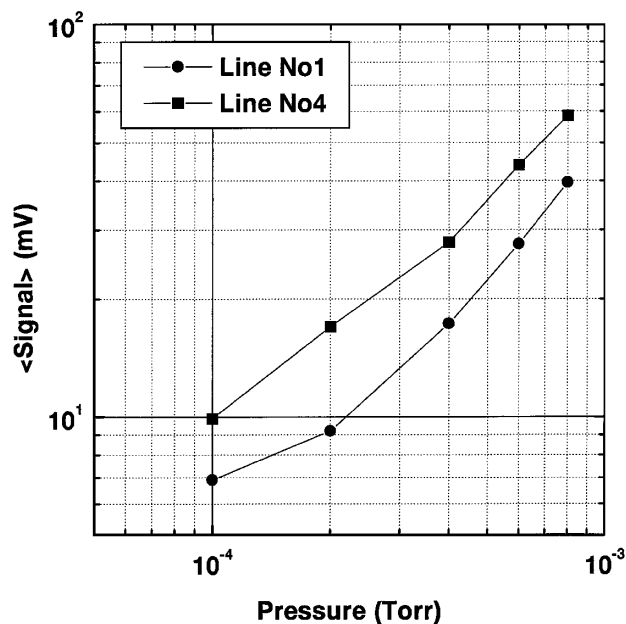


FIG. 4. Pressure dependence of several atomic nitrogen lines recorded at $\lambda = 800$ nm, $I = 10^{17}$ W/cm². The atomic nitrogen lines No1 and No4 are identified in Table I.

the protons following Coulomb explosion does not bring too much excitation to the remaining X^{Z+} ion. On the contrary, for molecules such as N_2 and N_2O the electronic density is delocalized and is shared by the atoms within the molecule. The Coulomb explosion of the system produces much more excitation of the fragments than in the XH_n system. Finally, the excitation in N_2O is much more important than in N_2 , following the line intensities reported in Table I. This experimental fact can be explained by the fact that the direct Coulomb explosion of a triatomic molecule into three fragments [8] involves more electrons than the Coulomb explosion of a diatomic molecule for the same final fragment charge states. This effect has been predicted for the linear H_3^+ triatomic molecular ion in comparison with H_2^+ in the frame of charge-resonance-

enhanced ionization [9]. Since N_2O is a linear molecule, the concepts developed in Ref. [9] for H_3^+ might be of importance for the more complicated N_2O molecule.

In conclusion, this Letter reports the first direct observation of excited states of transient multicharged molecules based on the experimental observation of excited fragments. The specificity of the molecular excitation is shown in comparison with similar experiments performed with rare gas atoms and is discussed as a function of the initial electronic configuration for NH_3 , N_2 , and N_2O . These processes are not well known and the present experimental results and future developments are expected to improve our knowledge of transient multicharged molecules produced by a strong laser field, as well as their very fast fragmentation dynamics [10].

The authors are pleased to acknowledge O. Gobert, P. Meynadier, and M. Perdrix for their expertise with the LUCA laser facility and M. Bougeard and E. Caprin for their skilled technical assistance.

-
- [1] K. Codling and L. J. Frasinski, *J. Phys. B* **26**, 783 (1993), and references therein.
 - [2] J. H. Posthumus, L. J. Frasinski, A. J. Giles, and K. Codling, *J. Phys. B* **28**, L349 (1995).
 - [3] T. Zuo and A. D. Bandrauk, *Phys. Rev. A* **52**, R2511 (1995).
 - [4] S. Chelkowski, T. Zuo, O. Atabek, and A. D. Bandrauk, *Phys. Rev. A* **52**, 2977 (1995).
 - [5] T. Seideman, M. Yu. Ivanov, and P. B. Corkum, *Phys. Rev. Lett.* **75**, 2819 (1995).
 - [6] M. Brewczyk, K. Rzazewski, and C. W. Clark, *Phys. Rev. Lett.* **78**, 191 (1997).
 - [7] W. C. Wiley and I. H. McLaren, *Rev. Sci. Instrum.* **26**, 1150 (1955).
 - [8] Ph. Hering and C. Cornaggia, *Phys. Rev. A* **59**, 2836 (1999).
 - [9] H. Yu and A. D. Bandrauk, *Phys. Rev. A* **56**, 685 (1997).
 - [10] A. D. Bandrauk, D. G. Musaev, and K. Morokuma, *Phys. Rev. A* **59**, 4309 (1999).